Zone Center Frequencies of Tetragonal CdAl$_2$Se$_4$

H. C. Gupta, Manoj Kumar Singh, and L. M. Tiwari

Physics Department, Indian Institute of Technology, Hauz Khas, New Delhi 110016, India

A short-range force constant and a modified rigid ion model have been applied for the first time to investigate the phonons in the CdAl$_2$Se$_4$ defect chalcopyrite compound in its tetragonal phase. The calculation with one bending and six stretching force constants in the short-range force constant model agrees well with the observed Raman and infrared frequencies. The Al–Se interatomic force constants of its bonds are found to be stronger than the Cd–Se interatomic force constants. In the modified rigid ion model, the effective charges have been incorporated along with the stretching and the bending force constants to exhibit a good agreement for the observed Raman and infrared frequencies. The effective charge on Cd cation has been found to be much smaller than the effective charge on Al cation. © 2000 Academic Press

INTRODUCTION

The $A^{II}B^{III}_2X^{VI}_4$ defect chalcopyrite ternary compounds have exhibited interesting technological applications in photoconduction, nonlinear optics, laser action, etc. Most of the earlier studies of such compounds were with $A^{II} =$ Cd, $B^{III}_2 =$ Ga or In, and $X^{VI}_4 =$ S or Se(1–7), but recently compounds with $A^{II} =$ Cd, $B^{III}_2 =$ Al, and $X^{VI}_4 =$ S or Se have been investigated in the band gap region for their optical properties and the lattice vibrational properties (8). Of the two, CdAl$_2$Se$_4$ was studied for the first time for the experimental Raman and infrared frequencies along with a preliminary theoretical investigation of Raman frequencies in terms of a simple Keating model. However, a detailed interatomic force constant analysis is required to interpret the observed Raman and infrared frequencies. Hence, in the present paper, we have investigated the optical phonons in CdAl$_2$Se$_4$ based on a short-range force constant and a modified rigid ion model. In the short-range force constant model (SRFCM), it is found that the nearest Al–Se bonds are stronger than the nearest Cd–Se bonds. Also, only the Al1–Se–Al2 bending interatomic force constant is effective in this compound. In the modified rigid ion model (MRIM), the effective ionic charge on Cd is found to be much smaller than the effective ionic charge on Al. Further, with the incorporation of these

effective charges in MRIM, all the nearest-neighbor dominant stretching force constants increase when compared with the corresponding values in the short range force constant model.

THEORY

CdAl$_2$Se$_4$ is a tetragonal crystal (space group $I\bar{4}$)characterized by a tetrahedral atomic configuration, in which two sides of the cationic lattice of a chalcopyrite structure are free, giving a defect chalcopyrite structure. The structure of defect chalcopyrite AB_2X_4 is shown in Fig. 1. The Cd–Se and the Al–Se bond lengths are respectively 2.63 and 2.402 Å (9).

At the center of the Brillouin zone, the vibrational spectrum is given by

$$\Gamma = 3A + 6B + 6E.$$

All the optical modes are Raman-active, and B and E (doubly degenerate) modes are also infrared-active.

The lattice dynamical calculations were carried out according to the Wilson-GF matrix method on the basis of cartesian symmetry coordinates (10). The dynamical matrix is given by

$$\mathbf{D} = \mathbf{M}^{-1/2}\mathbf{F}\mathbf{M}^{-1/2},$$

where $\mathbf{M}$ is a diagonal matrix specifying the masses of the atoms involved. The force constant matrix $\mathbf{F}$ is represented by the short-range stretching interactions with valence and repulsive force constants Ki and fi and the bending force constants Hi. In the present calculations with the short-range force constant model, we have used the three valence force constants, $K1$ (Al1–Se), $K2$ (Al2–Se), and $K3$ (Cd–Se); three repulsive force constants, $f1$ (Al1–Al2), $f2$ (Se–Se), and $f3$ (Se–Se); and one bending force constant, $H1$ (Al1–Se–Al2) as shown in Table 1.

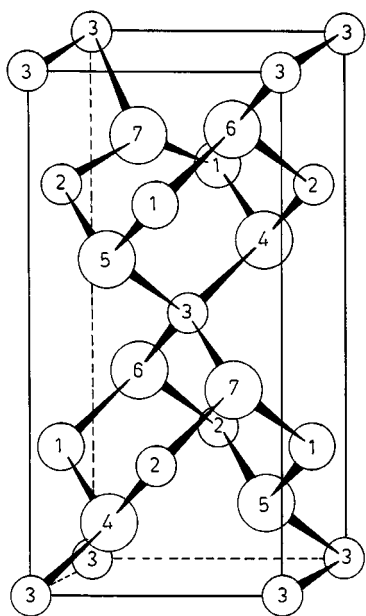In the modified rigid ion model, in addition to the seven force constants mentioned above, effective ionic charges

FIG. 1. Structure of defect chalcopyrite AB_2X_4 (1 = A atom; 2, 3 = B atom; 4, 5, 6, 7 = X atom).

TABLE 2
Symmetry Coordinates for Raman- and IR-Active Zone Center Phonons in Tetragonal CdAl₂Se₄ (4)

A	$q_1 = \frac{1}{2}(x_4 - x_5 + y_6 - y_7)$
	$q_2 = \frac{1}{2}(x_6 - x_7 - y_4 + y_5)$
	$q_3 = \frac{1}{2}(z_4 - z_5 - z_6 - z_7)$
B	$q_4 = z_1$
	$q_5 = z_2$
	$q_6 = z_3$
	$q_7 = \frac{1}{2}(x_6 - x_7 + y_4 - y_5)$
	$q_8 = \frac{1}{2}(x_4 - x_5 - y_6 + y_7)$
	$q_9 = \frac{1}{2}(z_4 + z_5 + z_6 + z_7)$
E	$q_{10} = x_1$
	$Q_{11} = x_2$
	$Q_{12} = x_3$
	$Q_{13} = \frac{1}{2}(x_4 + x_5 + x_6 + x_7)$
	$Q_{14} = \frac{1}{2}(y_4 + y_5 - y_6 - y_7)$
	$Q_{15} = \frac{1}{2}(z_4 - z_5 - z_6 + z_7)$

were used as follows: $Z^*_{Cd} = 0.2$, $Z^*_{Al} = 1.0$, and $Z^*_{Se} = -0.55$. These charges were obtained in such a manner that the w_{TO}–w_{LO} splitting in the infrared modes can be satisfactorily explained.

The input parameters are the unit cell dimensions, the fractional coordinates, the masses of the atoms, the symmetry coordinates as given in Table 2 (4), and the phonon frequencies (8). The interatomic force constants given in Table 1 were obtained by the best fits to the measured Raman and infrared frequencies.

was found to contribute to the optical phonons at the zone center. In addition, the nearest Al–Se force constants were larger than the nearest Cd–Se force constant. This is due to the Cd vacancies in the CdAl₂Se₄ defect chalcopyrite structure. It is due to this reason itself that the Cd–Cd repulsive force constant was negligible in the fitting process, whereas Al1–Al2 and Se–Se repulsive force constants have a contribution to the optical phonons. It is also evident from

RESULTS AND DISCUSSION

It is obvious from Table 1 of the interatomic force constants that only one bending force constant, Al1–Se–Al2,

TABLE 1
Interatomic Force Constant Values in CdAl₂Se₄

Interatomic interaction between	Force constant	Force constant value (in N/cm)	
		For SRFCM	For MRIM
Al1–Se	$K1$	1.041	1.276
Al2–Se	$K2$	0.861	1.013
Cd–Se	$K3$	0.649	0.743
Al1–Al2	$f1$	0.239	0.162
Se–Se	$f2$	0.127	0.074
Se–Se	$f3$	0.055	0.019
Al1–Se–Al2	$H1$	0.105	0.067

TABLE 3
Calculated Zone Center Raman and Infrared Frequencies (in cm⁻¹) in the Tetragonal Phase of CdAl₂Se₄ Compared to Experimental Values Obtained by Eifler et al. (8)

Species obtained	Present calculated values			Experimental values	
	SRFCM	MRIM			
		w_{TO}	w_{LO}	w_{TO}	w_{LO}
A	207.3	199.7		215	
	189.5	177.1		185	
	132.0	129.8		135.5	
B	376.7	379.9	384.8	377.5	392.5
	312.8	317.9	350.1	315	348
	197.2	195.7	198.7	197	203
	137.6	135.9	140.6	131.5	133.5
	80.0	89.2	91.8	80.0	81.5
E	376.4	382.2	401.9	373	402
	338.1	334.1	352.1	338.5	350.5
	178.1	183.9	184.3	178	185
	118.9	118.2	119.4	123.5	124
	75.0	80.4	80.5	67.5	71

Table 1 that in MRIM, the three dominant valence force constants increase, while the repulsive and the bending force constants decrease, when compared with SRFCM.

With these force constants, the calculated Raman and infrared frequencies at the zone center for CdAl$_2$Se$_4$ are given in Table 3. Also shown in Table 3 are the measured values of the Raman and infrared spectra (8). The present calculations in SRFCM with seven force constants provide a good agreement with the experimental values for Raman as well as infrared frequencies, whereas in MRIM, the agreement between theory and experiment is satisfactory except the lowest value in infrared modes. This discrepancy may be due to a large contribution from the Coulomb forces to the lowest wave number. It should be pointed out that in the MRIM, the effective charge on heavy Cd is found to be much smaller than the effective charge on lighter Al to explain the observed LO–TO splitting in the infrared modes.

The potential energy distributions for the Raman and the infrared modes for SRFCM and MRIM are presented in Table 4. The long-range force constant (LRFC) is found to be important at low wavenumbers. The force constant $K1$ generally dominates the largest wavenumbers for each of the species, whereas the next two largest wavenumbers in each species are more influenced by force constants $K2$ and $K3$, respectively. It is also observed that the repulsive force constant $f1$ between Al1–Al2 atoms does not contribute to Raman A modes, while the repulsive force constant $f2$

TABLE 4
Potential Energy Distributions of the Optical Zone Center Frequencies of CdAl$_2$Se$_4$

Species	Frequency (in cm^{-1})	Model	Force constant							
			$K1$	$K2$	$K3$	$f1$	$f2$	$f3$	$H1$	LRFC
$A(1)$	207.3	SRFCM	42.9	0.0	17.8	0.0	24.8	6.3	8.2	
	199.7	MRIM	57.3	0.1	22.1	0.0	15.6	2.4	5.0	− 2.5
$A(2)$	189.5	SRFCM	6.7	51.3	4.2	0.0	19.2	13.4	5.2	
	177.1	MRIM	8.2	67.4	8.9	0.0	11.3	5.8	3.9	− 5.5
$A(3)$	132.0	SRFCM	8.8	0.6	27.5	0.0	24.5	35.9	2.7	
	129.8	MRIM	12.0	3.5	25.7	0.0	17.7	11.9	3.0	26.2
$B(1)$	376.7	SRFCM	45.4	15.4	0.3	34.9	0.5	0.1	3.4	
	379.9	MRIM	61.0	12.9	0.3	22.5	0.3	0.0	2.1	0.9
	384.8	MRIM	75.3	2.2	0.1	17.1	0.3	0.1	1.6	3.3
$B(2)$	312.8	SRFCM	34.7	60.0	0.1	2.3	2.1	0.5	0.3	
	317.9	MRIM	32.4	74.8	0.0	2.9	0.8	0.1	0.4	− 11.4
	350.1	MRIM	6.9	73.8	0.2	8.2	0.3	0.0	0.9	9.7
$B(3)$	197.2	SRFCM	0.8	4.2	46.7	6.0	20.8	4.9	16.6	
	195.7	MRIM	1.8	3.1	64.1	2.8	11.1	1.5	8.1	7.5
	198.7	MRIM	4.5	0.5	63.3	2.7	11.1	1.6	7.2	9.1
$B(4)$	137.6	SRFCM	5.3	1.2	27.5	3.9	39.1	9.2	13.8	
	135.9	MRIM	3.6	8.8	13.2	3.4	28.2	3.9	13.1	25.8
	140.6	MRIM	0.9	16.1	6.5	3.2	28.7	4.0	13.1	27.5
$B(5)$	80.0	SRFCM	0.0	2.7	25.4	0.5	56.0	13.2	2.2	
	89.2	MRIM	1.9	0.4	23.3	0.8	26.6	3.7	2.6	40.7
	91.8	MRIM	5.0	0.0	29.7	1.1	22.3	3.1	3.4	35.4
$E(1)$	376.4	SRFCM	76.6	3.1	0.3	14.5	0.0	0.3	5.2	
	382.2	MRIM	93.5	1.4	0.4	8.6	0.0	0.1	3.8	− 7.8
	401.9	MRIM	80.5	4.3	0.6	3.1	0.0	0.1	6.0	5.4
$E(2)$	338.1	SRFCM	4.9	73.8	0.1	7.9	0.0	0.1	13.2	
	334.1	MRIM	2.5	91.4	0.1	6.9	0.0	0.0	7.9	4.2
	352.1	MRIM	7.1	78.3	0.0	12.4	0.0	0.1	3.8	− 1.7
$E(3)$	178.1	SRFCM	0.0	4.8	82.1	1.0	0.0	7.9	4.2	
	183.9	MRIM	0.1	5.5	89.7	0.4	0.0	2.3	2.1	− 0.1
	184.3	MRIM	0.3	6.4	88.8	0.4	0.0	2.3	1.9	− 0.1
$E(4)$	118.9	SRFCM	4.2	19.5	1.2	19.8	0.0	29.8	25.5	
	118.2	MRIM	8.1	26.3	0.2	11.8	0.0	10.6	15.3	27.7
	119.4	MRIM	10.6	23.9	0.0	11.9	0.0	10.5	14.7	28.4
$E(5)$	75.0	SRFCM	0.4	31.4	16.2	0.5	0.0	38.6	12.9	
	60.4	MRIM	0.2	30.2	10.4	1.2	0.0	12.7	10.0	35.3
	80.5	MRIM	0.2	30.2	10.6	1.2	0.0	12.7	10.0	35.1

between Se–Se atoms does not contribute to the infrared E modes.

REFERENCES

1. G. Krauss, V. Kramer, A. Eifler, V. Riede, and S. Wenger, *Cryst. Res. Technol.* **32,** 223 (1997).
2. J.-D. Hecht, A. Eifler, V. Riede, V. Schubert, M. Krauss, and V. Kramer, *Phys. Rev. B* **57,** 7037 (1998).
3. T. Y. Park, C. D. Kim, C. S. Yoon, D. I. Yang, H. J. Song, and W. T. Kim, *Inst. Phys. Conf. Ser.* **152,** 617 (1998).
4. H. Haeuseler, *J. Solid State Chem.* **26,** 367 (1978).
5. P. P. Lottici and C. Razzetti, *J. Phys. C* **16,** 3449 (1983).
6. P. W. Ohrendorf and H. Haeuseler, *J. Solid State Chem.* **114,** 442 (1995).
7. I. M. Tiginyanu, P. P. Lottici, C. Razzetti, and S. Gennari, *Jpn. J. Appl. Phys.* **32** (Suppl. 3), 561 (1993).
8. A. Eifler, J.-D. Hecht, V. Riede, G. Lippold, W. Schmitz, G. Krauss, V. Kramer, and W. Grill, *J. Phys. Condens. Mater.* **11,** 4821 (1999).
9. H. Neumann, *Cryst. Res. Technol.* **28,** 381 (1993).
10. T. Shimanouchi, M. Tsuiboi, and T. Miyazawa, *J. Chem. Phys.* **35,** 1597 (1961).